Molecular pharmacology

Supplementary Information

Pharmacology and Structure of Isolated Conformations of the Adenosine A_{2A} Receptor Define Ligand Efficacy

Kirstie A. Bennett, Benjamin Tehan, Guillaume Lebon, Christopher G. Tate, Malcolm Weir,

Fiona H. Marshall & Christopher J. Langmead

Heptares Therapeutics Ltd., Biopark, Broadwater Road, Welwyn Garden City, Hertfordshire, AL7 3AX

Supplementary Table 1. Summary of adenosine A_{2A} receptor constructs used in the study. Numbers in superscript refer to Ballesteros-Weinstein numbering.

Construct	Stabilising mutations	Conformation	Reference
A_{2A}	n/a	Wild-type	n/a
$A_{2A(1-316)}$	Removal of last 97 amino acids	Wild-type	(Robertson et al., 2011)
GL0	$L48A^{2.26}$	Active-state	(Lebon et al., 2011a)
GL23	$L48A^{2.26}$, $Q89A^{3.37}$, $T65A^{2.63}$	Active-state	(Lebon et al., 2011a)
GL26	$L48A^{2.26}$, $Q89A^{3.37}$, $T65A^{2.63}$, $A54L^{2.52}$	Active-state	(Lebon et al., 2011a)
GL31	$L48A^{2.26}$, $Q89A^{3.37}$, $T65A^{2.63}$, $A54L^{2.52}$, N154A*	Active-state	(Lebon et al., 2011b)
$StaR2_{(1-316)}$	Removal of last 97 amino acids, $A54L^{2.52}$, $T88A^{3.36}$, $K122A^{4.43}$, $V239A^{6.41}$, $R107A^{3.55}$, $L202A^{5.63}$, $L235A^{6.37}$, $S227A^{7.42}$	Inactive-state	(Robertson et al., 2011)

Supplementary Table 2: Affinity of [^{3}H]NECA at A_{2A}, $A_{2A(1-316)}$ and the active state StaRs (GL0, GL23, GL26, GL31). The affinity of [^{3}H]NECA at the A_{2A} receptor, $A_{2A\ (1-316)}$ and the full length A_{2A} StaRs was measured using saturation binding assays in CHO membranes transiently expressing each receptor. There was no significant difference in affinity of [^{3}H]NECA at A_{2A} and $A_{2A(1-316)}$ (P=0.51; unpaired two-tailed t-test). The affinity of [^{3}H]NECA was not significantly altered at the active state StaRs (P=0.15; one-way ANOVA), although the B_{max} was significantly increased at GL26 and GL31 compared to A_{2A} (P<0.05; one-way ANOVA with Dunnett's post-hoc test) and at $A_{2A(1-316)}$ compared to A_{2A} (P<0.01; unpaired two-tailed t-test). Data displayed as mean ± S.E.M from n= 3-8 experiments.

Construct	pK_D ± S.E.M	B_{max} (pmol/mg) ± S.E.M
A_{2A}	8.22 ± 0.16	3.28 ± 0.61
GL0	8.23 ± 0.09	9.42 ± 1.82
GL23	8.42 ± 0.10	12.96 ± 2.61
GL26	8.44 ± 0.11	18.80 ± 5.72*
GL31	8.73 ± 0.19	18.29 ± 5.54*
$A_{2A(1-316)}$	7.87 ± 0.02	7.53 ± 0.99**

Supplementary Table 3: Affinity of compounds measured using [^{3}H]NECA and [^{3}H]ZM241385 at the $A_{2A(1-316)}$. Measurement of affinity of agonist (NECA), neutral antagonists (theophylline and istradefylline) and inverse agonists (XAC, SCH58261) at the $A_{2A(1-316)}$ receptor as measured using the agonist radioligand [^{3}H]NECA and inverse agonist radioligand [^{3}H]ZM241385 (from Robertson et al., 2011). Data shown mean ± S.E.M from n=3.

Compound	pKi ± S.E.M measured using [^{3}H]ZM241385	pKi ± S.E.M measured using [^{3}H]NECA
NECA	7.0 ± 0.1	7.8 ± 0.2
Theophylline	5.2 ± 0.1	5.9 ± 0.1
Istradefylline	7.1 ± 0.1	7.1 ± 0.1
XAC	7.6 ± 0.1	8.6 ± 0.0
SCH58261	8.3 ± 0.0	8.9 ± 0.1

Supplementary Table 4: Potency of compounds in the functional assay as measured at 0.3 ng/mL doxycycline. Values below shown potency of inverse agonists/antagonists (pIC_{50}) and of agonist (pEC_{50}) in the cAMP assay. Data shown mean ± S.E.M from n=3.

	pIC_{50} ± S.E.M.
Istradefylline	8.43 ± 0.77
Theophylline	6.66 ± 0.48
Caffeine	5.90 ± 0.34
XAC	6.99 ± 0.50
SCH58261	8.00 ± 0.24
Preladenant	8.18 ± 0.32
ZM241385	8.67 ± 0.40
NECA	*pEC_{50} = 8.44 ± 0.32*

Supplementary Figure 1. **Responses of istradefylline, caffeine, ZM241385, SCH58261 and XAC at different levels of constitutive activity.** The responses of **A.** istradefylline, **B.** caffeine, **C.** ZM241385, **D.** SCH58261 and **E.** XAC were measured over different receptor densities (receptor expression induced by 0 ng/mL doxycycline (filled circles), 0.3 ng/mL doxycycline (filled squares) or 10 ng/mL doxycycline (filled triangles); 16 h) and hence different levels of constitutive activity. ZM241385, SCH58261 and XAC all acted as inverse agonists whilst theophylline and caffeine essentially acted as neutral antagonists. NECA response at each receptor density is shown as a dotted line to allow comparison to agonist response.

Supplementary Figure 2A. Overlay of the co-crystal structures both UK-432097 (PDB code: 3QAK) and NECA (PDB code: 2YDV) showing the surface of the NECA binding site in grey. UK-432097 is shown in pink; NECA is shown in green. **B.** As for **A.**, but including the surface of the UK-432097 binding site shown in pink. There are no significant differences in the surfaces of the two binding sites in the regions of interest.

Supplementary Figure 3. **ZM241385 sterically prevents movement of H250$^{6.52}$.** There is around a 2 Å inwards movement of H250$^{6.52}$ thought to accompany receptor activation as a result of the inward 'bulge' of TM5(Lebon et al., 2011b). **A.** Grey mesh surface shows extent of active-state binding pocket. ZM241385 structure is shown in spacefill and can be seen to protrude outside of the agonist binding site adjacent to H250$^{6.52}$. **B-D** Pink mesh surface shows extent of inactive-state binding pocket. **B.** Space fill of NECA shown within surfaces of both active- and inactive-state binding site. **C.** The inactive-state binding pocket protrudes towards H250$^{6.52}$ allowing ZM241385 to be fully accommodated within the inactive state binding pocket. **D.** Overlay of NECA (green) and ZM241385 (pink) structures where the compounds bind relative to one another.

Supplementary Figure 1

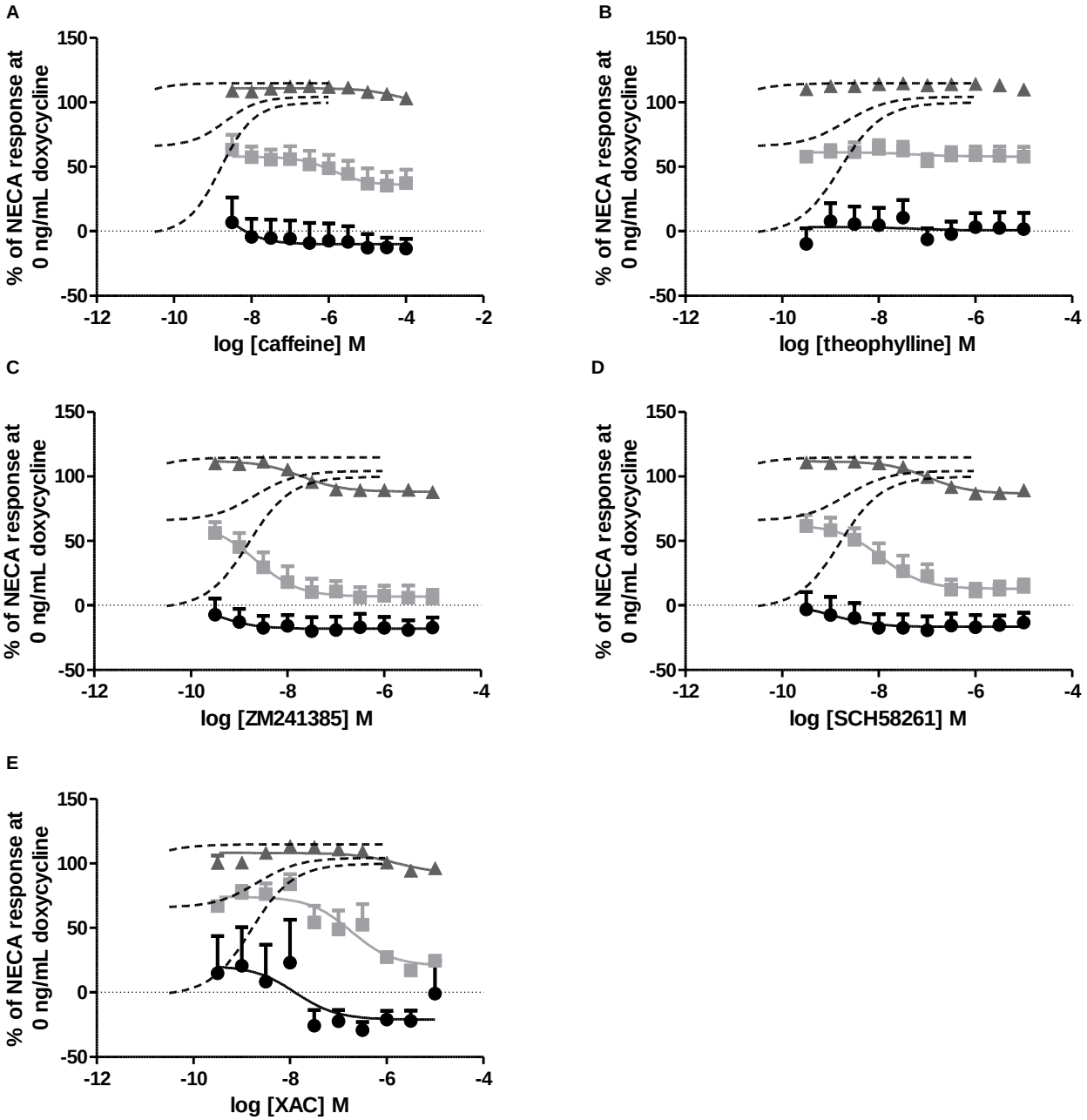

Supplementary Figure 2

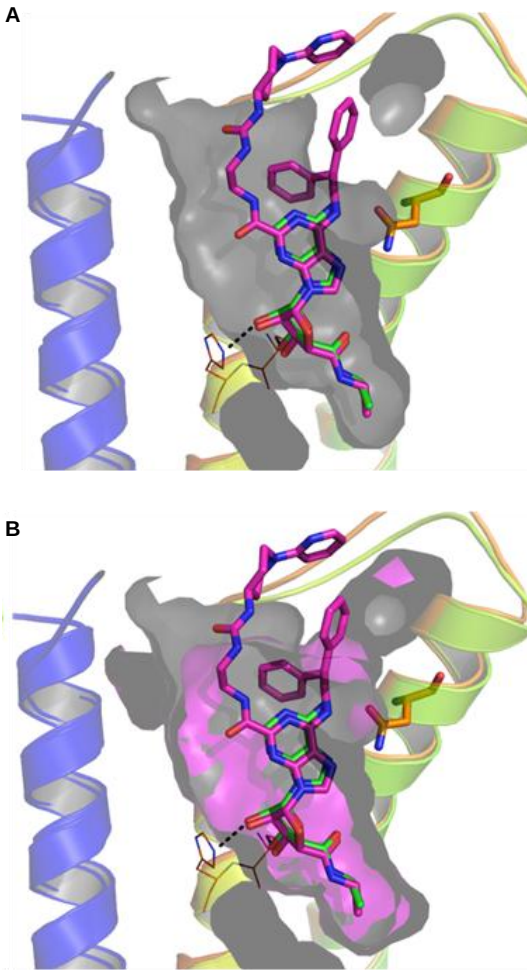

Supplementary Figure 3